JOURNAL OF MATERIALS SCIENCE 26 (1991) 4581–4587

Transport, magnetic and spectroscopic studies of nickel-gallium ferrites

A. AHMED, V. S. DARSHANE
Department of Chemistry, The Institute of Science, Bombay 400 032, India

X-ray, electrical conductivity, magnetic hysteresis and infrared spectroscopic studies for the system $NiGa_{2-2x}Fe_{2x}O_4$ were carried out. All the compounds, $0 \leqslant x \leqslant 1$ showed cubic symmetry. The activation energy, thermoelectric coefficient values decreased with increasing Fe^{3+} concentrations but with increasing number of Fe^{3+} ions, the values of lattice constant and magnetic moment increased. Compounds with $x \leqslant 0.5$ are p-type while those with $x \geqslant 0.75$ are n-type semiconductors. Magnetic hysteresis loops indicated that the compounds with $x \geqslant 0.25$ are ferrimagnetic while the compound $NiGa_2O_4$ ($x = 0.0$) is anti-ferromagnetic. Constant and low values of coercive force indicated that the compounds with $x \geqslant 0.50$ exhibit multidomain behaviour. X-ray intensity calculations, electrical conductivity, magnetic hysteresis and infrared studies indicate the presence of Ga^{3+} ions at the tetrahedral site, Ni^{2+} ions at the octahedral site and Fe^{3+} ions are present in both tetrahedral and octahedral sites. The probable ionic configuration for the system $NiGa_{2-2x}Fe_{2x}O_4$ is suggested to be $Ga^{3+}_{1-x}\,Fe^{3+}_{x}\,[Ni^{2+}\,Fe^{3+}]\,O^{2-}_4$.

1. Introduction

Oxidic spinels (AB_2O_4) have been studied by several workers [1, 2]. We have also reported our findings on various oxidic spinel systems [3–7]. These materials exhibit interesting structural, electrical and magnetic properties, which vary with the nature of the ions, their charge and site distributions amongst tetrahedral and octahedral sites in the lattice. Cation distribution depends on temperature and preparative methods. In spinels containing metals of the first transition series, the cation distribution cannot be determined by X-ray technique alone to any great accuracy because of the close atomic scattering powers of these ions. The present work attempted to overcome this problem by simultaneously using different techniques, such as X-ray, electrical conductivity, thermoelectric power, infrared and magnetic hysteresis.

A literature survey indicated that magnetic behaviour and structural investigations of various compounds of nickel ferrite-alumunates and nickel ferrite-gallates had been carried out by Maxwell and Pickart [8]; however, conclusions were not drawn using different techniques. In the present work, we prepared various compounds of the system $NiGa_{2-2x}Fe_{2x}O_4$ by a conventional ceramic technique by gradually substituting iron for gallium. The system was studied using X-ray, electrical conductivity, thermoelectric power, magnetic hysteresis and infrared spectroscopy in order to arrive at the probable ionic configuration.

2. Experimental procedure

2.1. Sample preparation

Different compositions of the system $NiGa_{2-2x}Fe_{2x}O_4$, ($x = 0.0$, 0.25, 0.50, 0.75 and 1.0) were prepared by mixing component oxides (GR grade) in acetone in appropriate molar proportions. The unreacted oxide mixture (after homogenizing) of each composition was subjected to thermogravimetric analysis (TGA, using MOM derivatograph) up to 1273 K. The loss in weight in all the compositions of the system was negligible (0.03%) suggesting that the compounds were sufficiently stoichiometric. Pellets of different compositions were prepared using polyvinylacetate as a binder. To remove the binder, the pellets were slowly heated at 773 K for 12 h and fired at 1173 K, sintering temperature, for 100 h. The samples were cooled in air at 50 K h^{-1}. The loss or addition of an element was further checked by weighing the samples before and after heating and in all cases the change was negligible.

2.2. Structural analysis

X-ray powder diffraction (XRD) patterns were recorded on a diffractometer (Siemens D-500, Kristalloflex) with a microprocessor controller, using CuK_α radiation ($\lambda = 0.15406$ nm) with a nickel filter to study the compounds both for lattice parameter and intensity measurements. All the X-ray patterns showed no lines other than those belonging to spinel structure. To measure the intensity, the height under different ($h\,k\,l$) peaks were determined and values obtained in relation to the peak height for the 3 1 1 reflection which was taken as 100. To ensure the reliability of the methods, the specimens were subjected to X-ray diffractometry twice and after correcting for background a mean value of area was taken. To calculate the relative integrated intensity of a given

0022–2461/91 $03.00 + .12

$(h\,k\,l)$ reflection, the following formula [9] was used

$$I = (F_{h\,k\,l})^2\, P\, L_P \qquad (1)$$

where F is the structure factor, P the multiplicity factor and L_P the Lorentz polarization factor. The atomic scattering powers for various ions were taken from the International Tables [10].

In spinels, the $(h\,k\,l)$ reflections for 2 2 0, 3 1 1, 2 2 2, 4 0 0, 4 2 2, and 4 4 0 were sensitive to cation distribution at both the sites. To determine the cation distribution and its variation with the composition, the intensity ratios $I_{4\,4\,0}/I_{4\,2\,2}$, $I_{2\,2\,0}/I_{4\,4\,0}$, $I_{4\,2\,2}/I_{4\,0\,0}$, $I_{3\,1\,1}/I_{2\,2\,0}$ and $I_{2\,2\,0}/I_{2\,2\,2}$ for different possible models of cation distribution were calculated and compared with the observed intensity ratios. The maximum standard deviation in the observed intensity ratio was $\pm$ 0.02. According to Bertaut [11] and Weil *et al.* [12] the best cation distribution is obtained when compared with experimental and theoretical intensity ratios for reflections whose intensities (i) are independent (or very slightly dependent) of oxygen parameter, U, (ii) vary with the inversion parameter in the opposite sense, and (iii) do not differ strongly. The above reflections and ratios were selected because they fulfil the requirements.

2.3. Transport studies

The d.c. electrical resistivity was measured using an LCR Marconi bridge. The end faces of each pellet were coated with a thin layer of conductive silver paste which was activated in an oven for 5 h. Resistivity was measured from room temperature to 773 K using a two probe technique; an electric field of 20 V cm^{-1} was applied across the pellets for these measurements. Thermoelectric power measurements were carried out after sandwiching a thick pellet between two copper blocks from room temperature to 503 K. The temperature difference across the sample was measured using a chromel–alumel thermocouple and the potential difference generated was measured using a microvoltmeter.

TABLE I Lattice constant, a, room temperature resistivity, ρ_{RT}, activation energy, ΔE, and thermo-electric coefficient values, α, for the system $NiGa_{2-2x}Fe_{2x}O_4$

Compounds	a(nm)	ρ_{RT}(Ω cm^{-1})	ΔE(eV)	α(μ V K^{-1})
$NiGa_2O_4$	0.8091	12.5×10^7	0.654	+368.99
$NiGa_{1.5}Fe_{0.5}O_4$	0.8198	1.2×10^7	0.490	+240.05
$NiGaFeO_4$	0.8222	8.4×10^6	0.450	+109.29
$NiGa_{0.5}Fe_{1.5}O_4$	0.8270	5.4×10^6	0.356	−91.82
$NiFe_2O_4$	0.8372	2.4×10^6	0.226	−133.52

2.4. Magnetic measurements

The magnetic hysteresis loops at room temperature (300 K) and at liquid nitrogen temperature (80 K) for all the ferrimagnets were taken on an alternating current electromagnet-type loop tracer, [13]. The saturation magnetization (σ_s) at 300 and 80 K was also measured on a digital multimeter. Magnetic hysteresis studies at room and liquid nitrogen temperatures were used to determine coercive force and domain behaviour of the compounds.

2.5. Infrared spectra

The IR spectra were recorded at room temperature on an IR spectrophotometer (Perken-Elmer 683) from 4000–200 cm^{-1}.

3. Results and discussion

3.1. Structural analysis

The lattice constants (a) for all the compounds of the system $NiGa_{2-2x}Fe_{2x}O_4$ are listed in Table I. All the compounds of the system are cubic. The lattice constants increased with increasing Fe^{3+} ion content in the crystal lattice. These values are in good agreement with the values reported earlier Maxwell and Pickart [8]. The increase in the lattice constant values may be due to replacement of smaller Ga^{3+} (0.062 nm) by larger Fe^{3+} ions (0.074 nm) at the tetrahedral site [14].

The cation distribution at the two tetrahedral and octahedral sites in the system $NiGa_{2-2x}Fe_{2x}O_4$ was

TABLE II Comparison of intensity ratios for the compounds $NiGa_2O_4$, $NiGaFeO_4$ and $NiFe_2O_4$ for the system $NiGa_{2-2x}Fe_{2x}O_4$

Cations at		$I_{4\,4\,0}/I_{4\,2\,2}$		$I_{2\,2\,0}/I_{4\,4\,0}$		$I_{4\,2\,2}/I_{4\,0\,0}$		$I_{3\,1\,1}/I_{4\,2\,2}$		$I_{2\,2\,0}/I_{4\,0\,0}$	
A-site	B-site	Obs.	Calc.	Obs.	Calc.	Obs.	Calc.	Obs.	Calc.	Obs.	Calc.
$NiGa_2O_4$											
Ga^{3+}	Ni_2^{2+}		3.574		0.699		0.799		8.439		1.996
Ga^{3+}	Ni^{2+}, Ga^{3+}		3.871		0.645		0.696		8.998		1.739
$Ni_{0.5}^{2+}$, $Ga_{0.5}^{3+}$	$Ga_{1.5}^{3+}$ $Ni_{0.5}^{2+}$	3.601	2.290	0.688	1.128	0.676	2.552	8.427	4.914	1.982	6.594
Ni^{2+}	Ga^{3+}, Ga^{3+}		2.642		1.016		1.712		5.563		4.597
$NiGaFeO_4$											
Ga^{3+}	Fe^{3+}, Ni^{2+}		3.375		0.729		0.887		7.806		2.175
$Ga_{0.5}^{3+}$ $Fe_{0.5}^{3+}$	$Ni_{0.5}^{2+}$, $Fe_{1.5}^{3+}$	3.298	5.001	0.715	0.505	0.862	0.399	7.708	11.605	1.996	1.008
Ni^{2+}	Ga^{3+}, Fe^{3+}		4.446		0.592		0.522		9.996		1.375
$NiFe_2O_4$											
Fe^{3+}	Ni^{2+}, Fe^{3+}		4.854		0.539		0.422		10.666		1.104
$Ni_{0.5}^{2+}$, $Fe_{0.5}^{3+}$	$Ni_{0.5}^{2+}$ $Fe_{1.5}^{3+}$	4.896	4.294	0.489	0.610	0.419	0.536	10.592	9.577	1.069	1.405
Ni^{2+}	Fe^{3+}, Fe^{3+}		3.827		0.685		0.656		8.660		1.719

investigated by X-ray intensity calculations. The observed and calculated intensity ratios for the different models of the compounds $NiGa_2O_4$ ($x = 0$), $NiGaFeO_4$ ($x = 0.5$) and $NiFe_2O_4$ ($x = 1.0$) are summarized in Table II and their diffraction patterns are given in Fig. 1. The various permutation and combinations of cationic arrangements between tetrahedral and octahedral sites have been taken using the site-preference energy data [15]. It is seen from Table II, that the models in which Ga^{3+} in $NiGa_2O_4$, Ga^{3+} and Fe^{3+} in $NiGaFeO_4$ and Fe^{3+} in $NiFe_2O_4$ compounds are present at A-sites show better agreement with the observed and calculated intensity ratios. These models are also further supported by site-preference energy data values [15]. It is not necessary to introduce a temperature correction into the intensity calculations because the oxide spinels have high melting points and thermal vibrations of atoms at room temperature should have negligible effect. A similar observation has been made by Datta and Roy [16] in $NiAl_2O_4$ and in other spinels.

3.2. Transport studies

D.c. resistivities of all the compositions of the system when measured as a function of temperature varied between 10^7 and 10 $\Omega\,cm^{-1}$. Plots of $\log\rho$ versus $10^3/T$ (Fig. 2), of all the compositions of the system were linear, indicating the semi-conducting nature of the compounds. Wilson's law $\rho = \rho_0 \exp(\Delta E/kT)$ was obeyed in all compositions. The activation energy

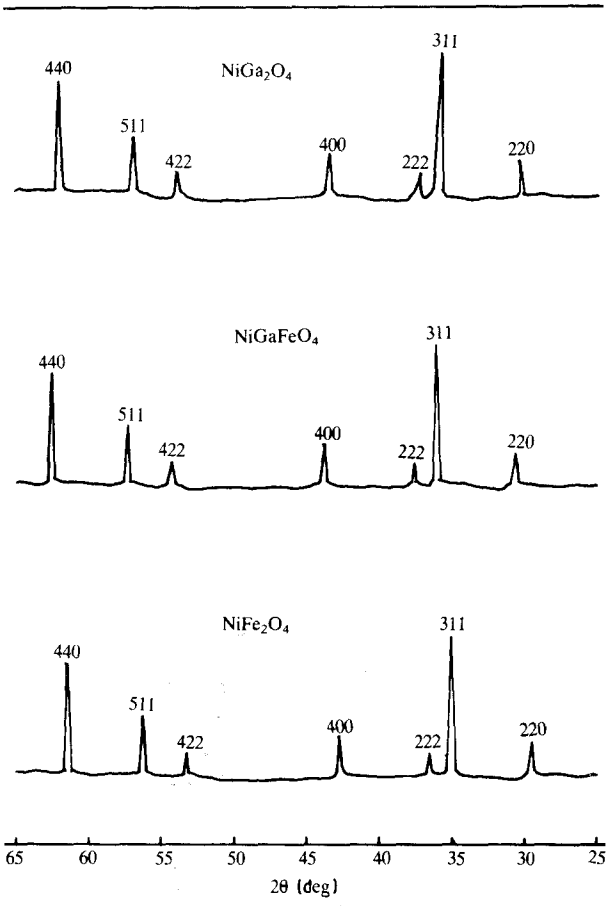

Figure 1 X-ray diffractometer patterns of compounds $NiGa_2O_4$, $NiGaFeO_4$ and $NiFe_2O_4$.

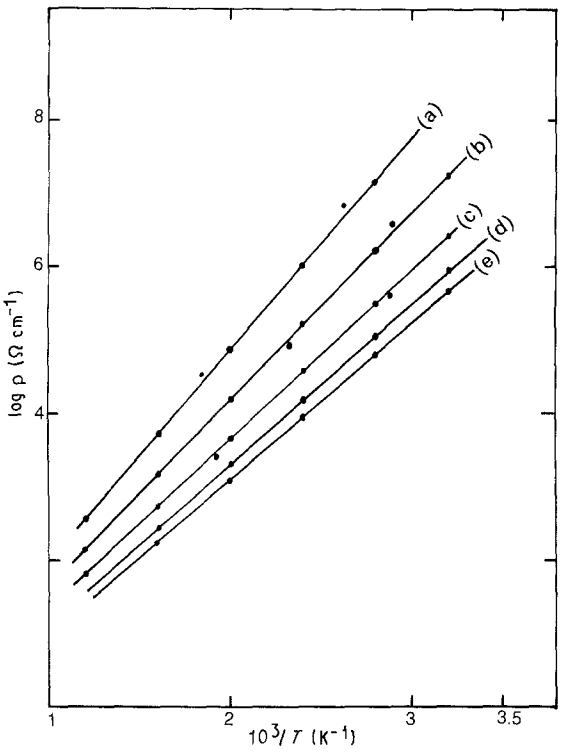

Figure 2 Plot of $\log\rho$ against $10^3/T$ for the system $NiGa_{2-2x}Fe_{2x}O_4$. (a) $x = 0.0$; (b) $x = 0.25$; (c) $x = 0.50$; (d) $x = 0.75$; (e) $x = 1.0$.

calculated from the slopes of the above plots for different compositions varied between 0.654 and 0.226 eV, as listed in Table I. Activation energy values were quite reproducible and maximum deviation was within the range of $\pm$ 0.01 eV. Plots of $\log\rho$ against $10^3/T$ show no break or inflection, indicating the presence of the stable oxidation states of all the cations over the temperature range studied. It can be seen from Table I that the values of activation energy slowly decreased from 0.654–0.226 eV as the concentration of Ga^{3+} decreased and that of Fe^{3+} increased. On substituting Fe^{3+} for Ga^{3+} ions in the crystal lattice the activation energy decreased due to the fact that completely filled Ga^{3+} (d^{10}) orbitals have much lower energy, i.e. they are very stable and are more contracted than the Fe^{3+} (d^5) orbitals. Also, as the concentration of Fe^{3+} ions increased in the lattice, the mobility of charge carriers increased, resulting in a gradual decrease in the activation energy. It is observed from Fig. 3, that the values of activation energy, ΔE, thermoelectric coefficient, α, and room-temperature resistivity, ρ_{RT}, decreased with decreasing Ga^{3+} concentration. This can be attributed to an increase in the number of charge carriers at the octahedral sites.

The electrical conductivity, σ, is related to the number of charge carriers, $n = n_e + n_h$, and their mobility, μ, at room temperature by the relation

$$\sigma = ne\mu \qquad (2)$$

where e is the electric charge; taking the average unit cell volume $(8.231)^3$ the value of hole concentration would be $1.4 \times 10^{22}\,cm^{-3}$ and the mobility value would be of the order of $10^{-9}\,cm^2\,V^{-1}\,s^{-1}$. Mobility can also be calculated using the equation of Heikes

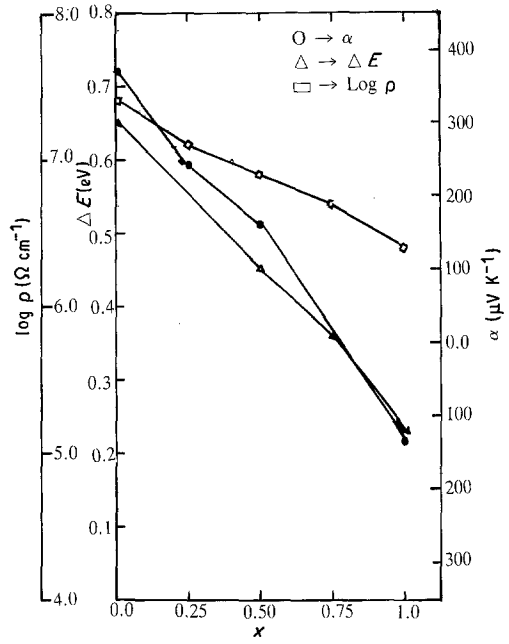

Figure 3 Plots of (□) room-temperature resistivity, log ρ, (Δ) activation energy, ΔE, and (○) thermoelectric coefficient, α, for the system $NiGa_{2-2x}Fe_{2x}O_4$.

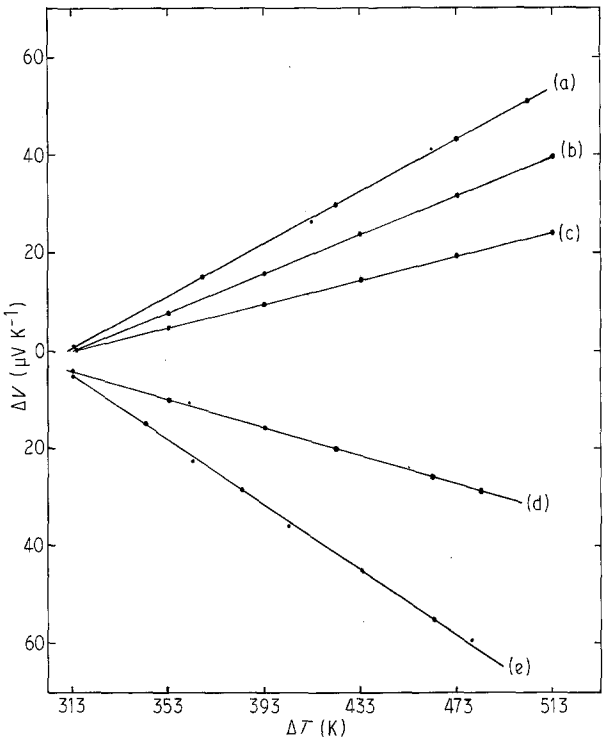

Figure 4 Plot of ΔV against ΔT for the system $NiGa_{2-2x}Fe_{2x}O_4$. (a) $x = 0.0$; (b) $x = 0.25$; (c) $x = 0.50$; (d), $x = 0.75$; (e) $x = 1.0$.

and Johnston [17]

$$\mu = ed^2\nu\exp(-\Delta E/KT)/KT \qquad (3)$$

where ΔE is the average activation energy, K the Boltzmann constant, d the jump length and ν the lattice frequency. The mobility value thus calculated using Equation 3 is 10^{-9} $cm^2 V^{-1} s^{-1}$. Infrared studies indicated the presence of two strong absorption bands at 450 and 600 cm^{-1}. These bands are due to intrinsic vibration of octahedral cations [18, 19]. However, the band at 600 cm^{-1}, being stronger than 450 cm^{-1}, was used for calculation of lattice frequency in Equation 3.

All compounds of the system possess low mobility values which increased exponentially with increasing temperature following the relationship

$$\mu = \mu_0\exp(-\Delta E/KT) \qquad (4)$$

where μ_0 is a constant representing the mobility at $T = \infty$. In the case of low mobility semiconductors and their exponential temperature dependence, the charge carriers are localized at a particular site and conduction involves the hopping of charge carriers from one site to another during lattice vibrations, therefore mobility shows an exponential temperature dependence.

Plots of thermo-e.m.f., ΔV, developed across the compounds against the temperature difference, ΔT, are given in Fig. 4. The thermoelectric coefficient, α, varied between + 368.99 and − 133.52 $\mu V K^{-1}$ as listed in Table I and plotted in Fig. 3. All the plots were linear obeying the equation suggested by Honig [20]

$$\alpha \pm = \frac{K}{e}\left(\ln\frac{1-S}{S} + \frac{\bar{S}_R}{K}\right) \qquad (5)$$

where S is the probability of cationic sites for extra charge carriers and $\bar{S}_R$ is the lattice relaxation entropy term. In the present system, $NiGa_{2-2x}Fe_{2x}O_4$, the gallium-rich compounds are p-type semi-conductors and the iron-rich compounds are n-type semiconductors [21]. Compounds with $x \leqslant 0.5$ of the system with a positive sign of α showed p-type semiconducting behaviour which can be attributed to the following process. In gallium-rich compounds, during the firing process, a very small amount of gallium may be lost and cation vacancies are created at the A-Site. As a result, a small number of B-site cations, Fe^{3+}, may go to the A-site creating holes at the B-site giving rise to p-type conduction. The value of thermoelectric power continues to decrease with increase in the concentration of Fe^{3+} at the B-sites, as the number of charge carriers decreases.

The compounds with $x \geqslant 0.75$ of the system with negative sign of α showed n-type semiconducting behaviour. In these compounds a slight oxygen deficiency is suspected due to the ability of Fe_2O_3 to lose oxygen when heated at elevated temperatures [22]. The oxygen non-stoichiometry will give rise to some Fe^{2+} ions in order to maintain electrical neutrality. Thus the following hopping mechanism is expected

$$Fe^{2+} + Fe^{3+} \rightleftharpoons Fe^{3+} + Fe^{2+} \qquad (6)$$

Therefore, we have small polaron-hopping charge carriers. The presence of Fe^{2+} ions could not be detected in the system. However, a very small concentration of Fe^{2+} cannot be ruled out as the compounds show n-type behaviour. As the concentration of Fe^{3+} increases in the system, the hopping process increases, thus both types of charge carrier are present in these compounds and the observed thermoelectric coefficient, α, results from the compensating effect of p-type and n-type charge carriers.

3.3. Magnetic properties

All the compounds of the system except $x = 0.0$ show magnetic hysteresis loops (M–H curves) at 300 and 80 K, Fig. 5. The coercive force, H_c, saturation magnetization, σ_s, and magnetic moment for ferrimagnetic compounds, are listed in Table III. The magnetic moment was calculated from the σ_s values at 80 K using the relation

$$n_B = \sigma_s \frac{\text{mol. wt}}{5585} \quad (7)$$

The observed n_B values obtained by using Equation 7 are compared with the calculated n_B values on the basis of spin-only moments, Table III.

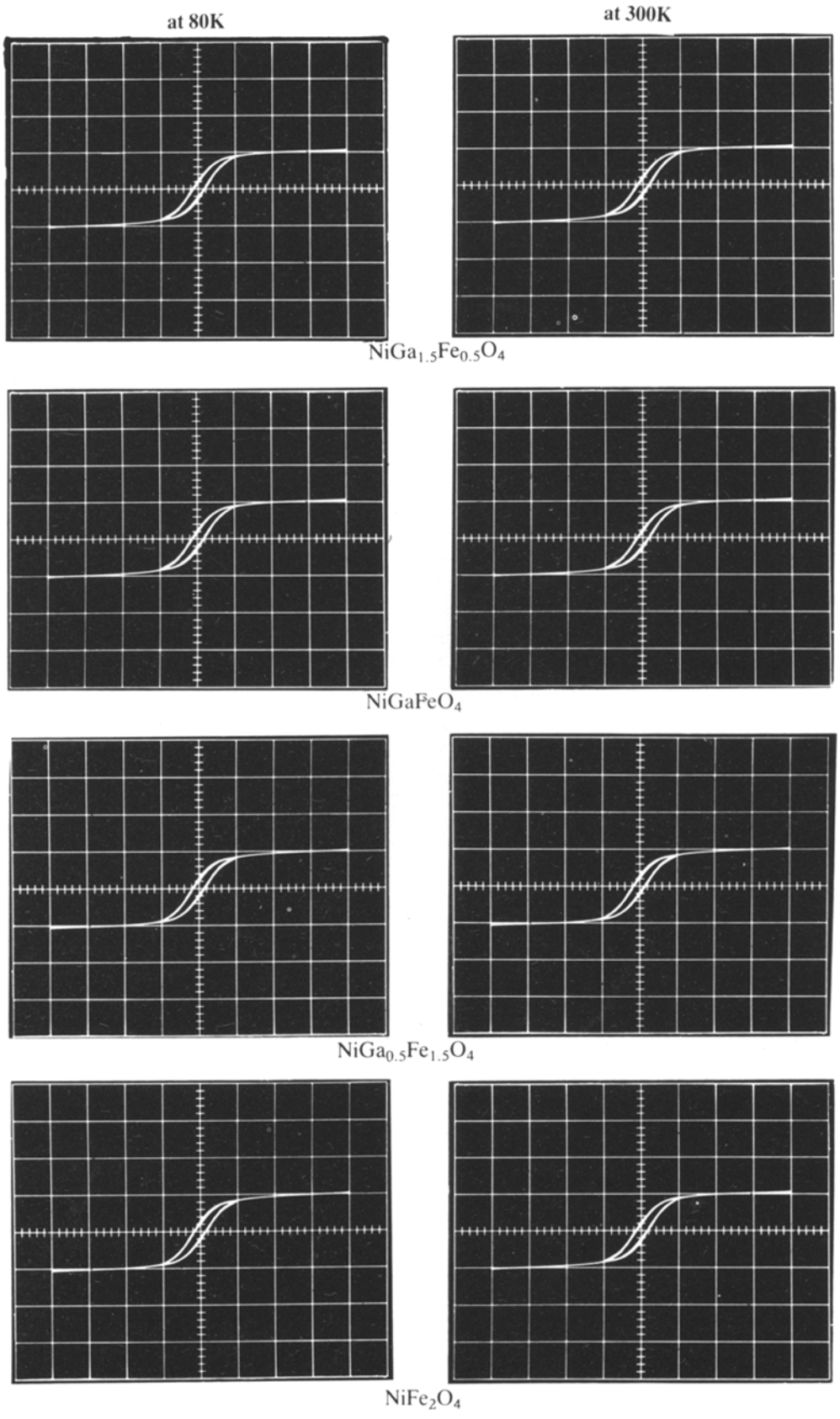

Figure 5 Hysteresis loops for the compounds of the system $NiGa_{2-2x}Fe_{2x}O_4$.

TABLE III Saturation magnetization, σ_s, coercive force, H_c, and magnetic moment, n_B, values for the system $NiGa_{2-2x}Fe_{2x}O_4$

Compound	H_c(Oe)		σ_s (e.m.u. g^{-1})		$n_B(\mu_B)$	
	300 K	80 K	300 K	80 K	obs.	calc.
$NiGa_2O_4$	–	–	–	–	–	–
$NiGa_{1.5}Fe_{0.5}O_4$	36	60	9.951	23.866	0.50	2.0
$NiGaFeO_4$	60	60	24.492	31.287	1.40	5.0
$NiGa_{0.5}Fe_{1.5}O_4$	60	60	56.413	52.155	2.20	4.5
$NiFe_2O_4$	60	60	57.716	73.931	2.0	2.10

The compound $NiGa_2O_4$ ($x = 0.0$) does not give any hysteresis loop at any applied field of 3 kOe even at 80 K, indicating that the magnetic ordering temperature is below 80 K.

From Table III, it can be seen that in the case of $NiFe_2O_4$ the observed and calculated magnetic moments shows close agreement indicating colinear behaviour. However, the low values of magnetic moment observed are also due to other magnetic interactions such as A–A and B–B interactions. It can be seen from the magnetic hysteresis loops (Fig. 5) that all the compounds except $NiGa_2O_4$ ($x = 0.0$) possess similar values of coercive force, H_c, at room temperature and at 80 K which may be due to the presence of anisotropy in these compounds. According to Takahashi and Fine [23], the rapid increase in the anisotropy constant on cooling is due to an increase in H_c with decreasing temperature. With decreasing temperature the compounds with $x \geqslant 0.50$ did not show any increase in H_c value indicating that there is no rapid increase in the anisotropy constant on cooling in these compounds. A large increase in H_c on cooling to 80 K is observed in $NiGa_{1.5}Fe_{0.5}O_4$, ($x = 0.25$), indicative of single-domain (SD) behaviour [24]. Such a large increase in H_c is not observed in compounds with $x \geqslant 0.50$ of the system attributed to multi-domain (MD) behaviour.

3.4. Infrared spectra

As mentioned earlier, all the compounds show two strong bands at about 600 and 450 cm^{-1} (Fig. 6). The band positions and the threshold frequency are listed in Table IV. The threshold frequency for the electronic transition was found to decrease with increasing Fe^{3+} concentration. This is in agreement with the trend observed for the activation energy, ΔE, as seen from Table I.

Tarte and Collongues [25] have observed that in normal ferrites, both absorption bands depend on the nature of octahedral cations and do not significantly depend upon the nature of tetrahedral ions. However, Waldron [26] and Hafner [27] attributed the band ν_1 at $\sim 600\ cm^{-1}$ to the intrinsic vibrations of tetrahedral complexes, and band ν_2 at $\sim 400\ cm^{-1}$ to that of octahedral complexes. The difference in band positions is because of the difference in the $Fe^{3+}O^{2-}$ distance for the octahedral and tetrahedral complexes. The presence of Fe^{2+} ions in the ferrites causes a shoulder or splitting of the absorption band [28]. In our compounds, neither of the bands shows shoulder or splitting, indicating the absence of Fe^{2+} ions.

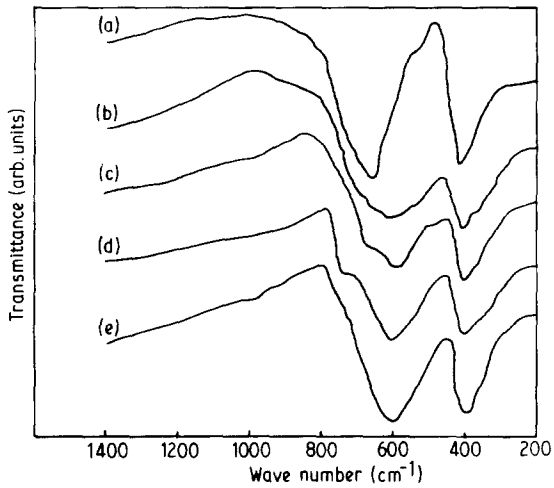

Figure 6 IR spectra of the system $NiGa_{2-2x}Fe_{2x}O_4$. x: (a) 0.0, (b) 0.25, (c) 0.50, (d) 0.75, (e) 1.0.

TABLE IV IR bands and threshold frequencies for the system $NiGa_{2-2x}Fe_{2x}O_4$

Compound	Absorption bands (cm^{-1})		
	ν_1	ν_2	Threshold frequency (cm^{-1})
$NiGa_2O_4$	670	430	1045
$NiGa_{1.5}Fe_{0.5}O_4$	640	415	950
$NiGaFeO_4$	590	415	880
$NiGa_{0.5}Fe_{1.5}O_4$	585	408	820
$NiFe_2O_4$	585	408	780

Thus X-ray, transport, magnetic and spectroscopic studies, suggest the probable cation distribution for the system $NiGa_{2-2x}Fe_{2x}O_4$ to be $Ga^{3+}_{1-x}Fe^{3+}_x$ $[Ni^{2+}\ Fe^{3+}]O^{2-}_4$.

References

1. J. B. GOODENOUGH, "Magnetism and Chemical Bond" (Wiley, New York, London, 1963) p. 120.
2. K.-H. HELLWEGE (ed), "Landolt-Bornstein, New series, Group III", Vol. 4b (Springer, Berlin, 1970).
3. M. N. KHAN, S. AL-DALLAL and A. AHMED, in "Proceedings of the International conference on Effects of modes of formation on the structure of glass. Diffusion and defect data" Vols 53–54 edited by R. A. Week, D. L. Kinser (Trans Tech publications, 1987) p. 409.
4. M. N. KHAN, A. AHMED and V. S. DARSHANE, *J. Mater. Sci.* **24** (1989) 163.
5. *Idem, ibid.* **24** (1989) 2615.

6. M. N. KHAN, S. AL-DALLAL, A. MEMON, A. AHMED and V. S. DARSHANE, *Mod. Phys. Lett. B* **3** (1989) 829.
7. S. AL-DALLAL, M. N. KHAN and A. AHMED, *J. Mater. Sci.*, **25** (1990) 407–410.
8. L. R. MAXWELL and S. J. PICKART, *Phys. Rev.* **92** (1953) 1120.
9. M. J. BUERGER, "Crystal structure analysis" (Wiley, New York, 1960) p. 46.
10. "International Tables for X-ray Crystallography", vol. 4 (Kynoch, Birmingham, 1974) p. 72.
11. E. F. BERTAUT, *Compt. Rend.* **230** (1950) 213.
12. L. WEIL, E. F. BERTAUT and L. BOCHIROL, *J. Phys. Rad.* **11** (1950) 208.
13. S. D. LIKHITE, C. RADHAKRISNAMURTY and P. W. SAHASRABUDHE, *Rev. Sci. Instrum.* **30** (1965) 1558.
14. R. D. SHANNON and C. T. PREWITT, *Acta Crystallogr. B* **26** (1970) 1076.
15. A. MILLER, *J. Appl. Phys.* **30** (suppl) (1959) 245.
16. R. K. DATTA and R. ROY, *J. Amer. Ceram. Soc.* **50** (1967) 578.
17. R. R. HEIKES and W. D. JOHNSTON, *J. Chim. Phys.* **26** (1957) 582.
18. P. TARTE, *Spectrochem. Acta* **19** (1965) 49.
19. P. S. JAIN and V. S. DARSHANE, *Ind. J. Chem.* **A19** (1980) 1050.
20. J. M. HONIG, *J. Chem Educ.* **43** (1966) 76.
21. G. H. JONKER, *J. Phys. Chem. Solids* **9** (1959) 165.
22. J. A. KULKARNI, K. MURALEDHARAN, J. K. SRIVASTAVA, V. R. MARATHE, V. S. DARSHANE, C. R. K. MURTHY and R. VIJAYARAGHAVAN, *J. Phys. C. Solid State Phys.* **18** (1985) 2593.
23. M. TAKAHASHI and M. E. FINE, *J. Appl. Phys.* **43** (1972) 4205.
24. R. VENKATESH and H. V. KEER, *Pramana. J. Phys.* **19** (1982) 103.
25. P. TARTE and R. COLLONGUES, *Ann. Chim (Fr.)* **9** (1964) 135.
26. R. D. WALDRON, *Phys. Rev.* **99** (1955) 1727.
27. S. HAFNER, *Z. Kristallogr.* **115** (1961) 331.
28. V. R. K. MURTHY, S. CHITRASANKAR, K. V. REDDY and J. SOBHANADRI, *Ind. J. Pure. Appl. Phys.* **16** (1978) 79.

Received 7 March
and accepted 29 October 1990